



Khan, A., Glaubes, H., Kent, A., Harrison, T., Foulds, A., Percival, C. J., & Shallcross, D. (2017). An estimate of the global budget and distribution of ethanol using a global 3-D atmospheric chemistry transport model STOCHEM-CRI. *Transactions of the Royal Society of South Africa*, 72(2), 174-183.
<https://doi.org/10.1080/0035919X.2016.1274276>

Peer reviewed version

Link to published version (if available):
[10.1080/0035919X.2016.1274276](https://doi.org/10.1080/0035919X.2016.1274276)

[Link to publication record on the Bristol Research Portal](#)
PDF-document

This is the author accepted manuscript (AAM). The final published version (version of record) is available online via Taylor & Francis at <http://www.tandfonline.com/doi/full/10.1080/0035919X.2016.1274276>. Please refer to any applicable terms of use of the publisher.

University of Bristol – Bristol Research Portal

General rights

This document is made available in accordance with publisher policies. Please cite only the published version using the reference above. Full terms of use are available:
<http://www.bristol.ac.uk/red/research-policy/pure/user-guides/brp-terms/>

1 **An estimate of the global budget and distribution of ethanol using a global 3-D**
2 **atmospheric chemistry transport model STOCHEM-CRI**

3
4 M. A. H. Khan¹, H. Glaubes¹, A. Kent¹, T. G. Harrison¹, A. Foulds¹, C. J. Percival²,
5 D. E. Shallcross^{1*}

6
7 ¹School of Chemistry, Cantock's Close, University of Bristol, BS8 1TS, UK

8 ²The School of Earth, Atmospheric and Environmental Science, The University of
9 Manchester, Manchester M13 9PL, UK

10 *Author for correspondence E-mail: d.e.shallcross@bristol.ac.uk

11
12
13
14
15
16
17
18
19
20
21
22
23
24
25
26
27
28
29
30
31
32
33
34
35
36
37
38
39
40
41
42
43
44
45
46
47
48
49
50

51 **An estimate of the global budget and distribution of ethanol using a global 3-D**
52 **atmospheric chemistry transport model STOCHEM-CRI**

53

54 **Abstract**

55 The atmospheric global budget and distribution of ethanol have been investigated using
56 a global three-dimensional chemistry transport model, STOCHEM-CRI. Ethanol, a
57 precursor to acetaldehyde and peroxy acetyl nitrate (PAN), is found throughout the
58 troposphere with a global burden of 0.024 to 0.25 Tg. The atmospheric lifetime of
59 ethanol is found to be 1.1 to 2.8 days, which is in excellent agreement with estimates
60 established by previous studies. The main global source of ethanol is from direct
61 emission (99%) and the remainder (1%) being produced via peroxy radical reactions.
62 In terms of removal rates of ethanol in the atmosphere, oxidation by hydroxyl radical
63 (OH) accounted for 51%, dry deposition 8% and wet deposition accounted for 41%.
64 Globally there are significant concentrations of ethanol over equatorial Africa, North
65 America and parts of Asia with considerably higher concentrations modelled over Saudi
66 Arabia and Eastern Canada. Through comparison of measured and modelled ethanol
67 data, it is apparent that the underestimation of the source strength of ethanol and the
68 coarse resolution of STOCHEM-CRI model produce the discrepancies between the
69 model and the measured data mostly in urban areas. The increased vegetation and
70 anthropogenic emissions of ethanol leads to an increase in the production of
71 acetaldehyde (by up to 90%) and peroxyacetyl nitrate (by up to 10%) which disrupts
72 the NO_x-ozone balance, promoting ozone production (by up to 1.4%) in the equatorial
73 regions.

74 **Keywords:** Global burden; atmospheric lifetime; chemistry transport model;
75 equatorial region; urban areas

76

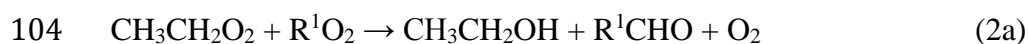
77 **INTRODUCTION**

78 Ethanol (C₂H₅OH) is recognized as a minor biogenic volatile organic compound
79 (BVOC) in the atmosphere, which can act as a precursor to acetaldehyde (CH₃CHO),
80 peroxyacetyl nitrate (PAN), and secondary aerosols (Blando and Turpin, 2000; Millet
81 *et al.*, 2012; Suarez-Bertoa *et al.*, 2015). Thus the changing of ethanol concentrations
82 has the potential to affect air pollution by changing the atmospheric composition and
83 chemistry.

84

85 Ethanol is emitted directly to the atmosphere from living plants, decaying plants,
 86 anthropogenic production, and biomass burning. The biogenic emissions are supposed
 87 to constitute the largest fraction of the global source of ethanol (Kirstine and Galbally,
 88 2012; Millet *et al.*, 2010; Naik *et al.*, 2010; Guenther *et al.*, 2012). The oceans may act
 89 either as a sink or as a source of ethanol, but fresh water regions may be net sinks of
 90 ethanol (Kirstine and Galbally, 2012; Avery *et al.*, 2016). Ethanol is also emitted
 91 anthropogenically because of its recent significant use as the biofuel in the fuel industry
 92 (Balat and Balat, 2009; Dunmore *et al.*, 2016). The usage of biofuels has been shown
 93 to exhibit higher levels of acetaldehyde within regions with high bio-ethanol and it has
 94 been suggested that urban levels could increase by up to 650% when 85% ethanol is
 95 incorporated into fuel (Sundvor and López-Aparicio, 2014). Jacobson (2007) showed
 96 that the incorporation of 85% ethanol in fuel resulted in the elevated levels of ozone
 97 and PAN. Within some areas 100% ethanol is used as a fuel source, such as Brazil
 98 where 20% of all vehicles run off pure ethanol (Lee, 2013). Photochemical production
 99 is another minor source of ethanol in where they are produced by the reaction of ethyl
 100 peroxy radicals ($\text{CH}_3\text{CH}_2\text{O}_2$; mainly produced from oxidation of atmospheric species
 101 such as ethane) with itself and other higher organic peroxy radicals (RO_2).

102



106

107 The loss due to OH oxidation is the main sink for atmospheric ethanol (Atkinson *et al.*,
 108 2006). The other removal processes including dry deposition and wet removal have
 109 been previously estimated to account for 23-35% of the total global sink (Millet *et al.*,
 110 2010; Naik *et al.*, 2010). The overall atmospheric lifetimes for ethanol in respect to the
 111 gross oceanic uptake, OH, and deposition are approximately 2-10 days (Atkinson *et al.*,
 112 2006; Naik *et al.*, 2010).

113

114 There are large regional differences in the atmospheric ethanol concentrations due to
 115 the wide variation in biogenic and anthropogenic contributions (Naik *et al.*, 2010). The
 116 increasing use of biofuels globally has made ethanol more important to understand how
 117 it affects the atmosphere and what implications this has to human health and also to the
 118 climate of the earth. Currently, there is uncertainty in emission literature data for

119 ethanol, which makes it challenging to model global atmospheric ethanol accurately. In
120 this study, we employ STOCHEM-CRI, a 3-dimensional global chemistry and transport
121 model to evaluate the global budget and the global distribution of tropospheric ethanol
122 after considering the updated emission data adapted from Naik *et al.* (2010) and
123 Kirstine and Galbally (2012). This work provides a good indication of the major issues
124 currently residing within the model and the current estimates of atmospheric ethanol.

125

126 **MODEL DESCRIPTION**

127 STOCHEM used in this study, is a global 3-dimensional Lagrangian Chemistry
128 Transport Model (CTM) first proposed by Collins *et al.* (1997). The model splits the
129 troposphere into 50,000 constant mass air parcels which works offline, incorporating
130 archived meteorological data to determine the transport of these parcels. The archived
131 data has a resolution of 1.25° longitude by 0.83° latitude with 12 uneven vertical levels
132 and includes information on the following: atmospheric temperature, pressure, wind
133 fields, cloud cover, precipitation and atmospheric boundary layer heights. A detailed
134 description of the vertical coordinate, advection scheme, convection and inter-parcel
135 mixing, and boundary layer used in STOCHEM can be found in Collins *et al.* (1997)
136 with updates described by Derwent *et al.* (2008). The chemical mechanism used in
137 STOCHEM, is the common representative intermediates mechanism version 2 and
138 reduction 5 (CRI v2-R5), referred to as ‘STOCHEM-CRI’ which is uncoupled from the
139 transport mechanism. The detail of the CRI v2-R5 mechanism is given by Watson *et al.*
140 *et al.* (2008) with updates highlighted in Jenkin *et al.* (2008) and Utembe *et al.* (2010). In
141 this study, CRI v2-R5 mechanism is further updated which consists of methane and 24
142 emitted non-methane hydrocarbons using 229 chemical species competing in 529 gas
143 phase reactions and 96 photolytic reactions and gives excellent agreement with the
144 MCM v3.1 over a full range of NO_x levels (Watson *et al.*, 2008; Jenkin *et al.*, 2008).
145 The photolysis rate was calculated explicitly for each air parcel. Ideally the model
146 should perform the calculation for each air parcel for every five minutes to match the
147 gas phase chemistry, but to save computational resources and time, the photolysis rate
148 was calculated at a time resolution of one hour, and then linearly interpolated with
149 respect to time to achieve the five minute resolution values which were used in the
150 chemical integration. The surface emissions (e.g. anthropogenic, biomass burning,
151 ocean, soil, vegetation) data employed in the base case STOCHEM model were
152 obtained from the Precursor of Ozone and their Effects in the Troposphere (POET)

153 inventory for NMVOCs (Granier *et al.*, 2005). Emissions are mapped 2-dimensionally
154 with a resolution of 5° longitude by 5° latitude monthly. Stratospheric tropospheric
155 exchange has been represented by incorporating the movement of ozone and nitric acid
156 into the highest level of the model using wind field data and ozone fields. Lightning
157 and aircraft emissions are accounted for as a three-dimensional emission and distributed
158 regularly between the convective cloud top height and the surface. Dry deposition is
159 one of the removal processes for atmospheric species which is accounted in the model
160 via gravitation movement process over land or oceans, with Antarctica and sea ice being
161 included as an ocean deposition processes and land ice being a terrestrial dry deposition
162 process. The wet deposition is represented by both convective and dynamic scavenging
163 coefficients which are species specific. The coefficients along with both precipitation
164 rates and scavenging profiles are used to determine loss rates of species in an air parcel
165 via this process. The simulation was conducted with meteorology from 1998 for a
166 period of 24 months with the first 12 allowing the model to spin up. Analysis is
167 performed on the subsequent 12 months of data. The three simulations were performed
168 which were based on the scenario in which the model was run with different global
169 ethanol emission values (Table 1). The dry deposition velocities over land and ocean
170 were considered as 1.6 and 3.0 mm/s, respectively which were used in all simulations.
171 Another simulation was performed using the emission class data by Naik *et al.* (2010),
172 with the inclusion of wet deposition parameters such as, dynamic scavenging of 2.0 cm^{-1}
173 ¹ and convective scavenging of 3.9 cm^{-1} determined using Henry's law coefficients
174 (Sander, 2015).

175

176 **RESULTS AND DISCUSSION**

177 Table 2 shows the global budget of ethanol produced by the STOCHEM-CRI. In the
178 base case (Run 1), the atmospheric sources of ethanol (3.2 Tg/yr) are found to be lower
179 than the studies of Naik *et al.* (2010) and Kirstine and Galbally (2012) since vegetation
180 sources were not included in the model. After adding vegetation emissions and
181 extended anthropogenic emissions in the model (Run 2), the estimated source strength
182 of 14.8 Tg/yr and the contribution of direct emission sources of 99% and photochemical
183 production sources of 1% are found which to lie within previous estimations regarding
184 ethanol emissions (Singh *et al.*, 2004; Naik *et al.*, 2010). The global ethanol emissions
185 determined for Run 3 (41.5 Tg/yr) was found to be much higher than Naik *et al.* (2010)
186 and Singh *et al.* (2004) which is due to the model incorporating a much larger flux value

187 for vegetation. The atmospheric source of ethanol from peroxy radicals for all of the
188 simulations was calculated to be a very small amount of 0.13 Tg/yr. Previous models
189 have shown large variations of the atmospheric sources of ethanol with estimations of
190 0.06 Tg/yr (Naik *et al.*, 2010), 0.5 Tg/yr (Kirstine and Galbally, 2012), and 2 Tg/yr
191 (Singh *et al.*, 2004). Larger species are capable of producing peroxy radical species
192 which are currently not being accounted for within the model, resulting in an under-
193 prediction for this value. The lack of kinetic data of the reaction between larger peroxy
194 radicals in the model also underestimate the photochemical production of ethanol.

195

196 The global sink of ethanol is dominated by OH oxidation (80-88%), with the remaining
197 contribution from dry deposition. However including wet deposition into STOCHEM
198 model (Run 4), the global sink contributions of ethanol accounted for a much larger
199 dependence on wet deposition with a ratio of 51:8:41 for OH oxidation, dry deposition
200 and wet deposition, respectively. Previous models have reported the respective ratios
201 of the losses by OH oxidation, dry deposition and wet deposition as 65:25:10 (Naik *et*
202 *al.*, 2010) and 75:21:4 (Kirstine and Galbally, 2012). The higher wet deposition loss of
203 ethanol is found in our model study which may be due to using the overestimated
204 scavenging coefficients in the model. The global burden (0.024 to 0.25 Tg) and lifetime
205 (1.1 to 2.8 days) of ethanol found in this study are well within the model results of Naik
206 *et al.* (2010) and Singh *et al.* (2004) (Table 2). The modelled global burden and lifetime
207 of ethanol decrease substantially when wet deposition is added into the simulation (Run
208 4), which is likely to be due to wet deposition potentially being a large and strong
209 removal process for ethanol.

210

211 Figure 1 shows the global distribution profiles for the average concentration of ethanol
212 for base case during June-July-August (J-J-A) and December-January-February (D-J-
213 F). In D-J-F, there is a higher level of ethanol, up to 300 ppt, over North America and
214 Saudi Arabia (Fig. 1b), likely due to the build-up of anthropogenic pollution in these
215 regions. Comparing with D-J-F, the intensity of ethanol is reduced significantly over
216 North America and Saudi Arabia during J-J-A due to the abundances of OH. The higher
217 concentrations of ethanol (up to 300 ppt) are present over Canada during J-J-A, this
218 could be due to the westerly winds resulting in a small proportion of pollution being
219 transported towards the Atlantic. Compared with D-J-F, the OH lifetimes of ethanol in
220 J-J-A are low near the equator due to the higher oxidation of ethanol by OH (Fig. 1c

221 and Fig. 1d). The spread of biofuel emissions was shown to be higher over North
222 America, South America, India and South-west Asia (Naik *et al.*, 2010) which were
223 reflected in the higher ethanol levels (up to 80 ppt) over North America, India and
224 South-west Asia. South America, from this model, appears to have low emission levels
225 of ethanol, which is unexpected as Brazil is one of the largest biofuel users after the
226 USA and the abundances of vegetation in tropical rainforests (Balat and Balat, 2009).
227 The absence of vegetation and the strong removal processes by OH concentrations
228 (especially in the summer time, D-J-F) in the base case result in lower ethanol
229 concentrations. After including vegetation emission, increased anthropogenic
230 emissions and biomass burning into the model (Run 2), the ethanol mixing ratios were
231 increased to 500 ppt in North America and Saudi Arabia and 300 ppt in tropical South
232 America and Africa (Fig. 1e and Fig. 1f). The high levels of ethanol present over South
233 America and Africa are likely to be produced via vegetation but also due to a large
234 amount of biomass burning occurring within these regions. The year used for the model
235 is 1998, an El Niño year, which causes intensified precipitation along Equatorial Africa
236 during the rainy season (October-November-December) potentially inducing more
237 stress and anaerobic respiration to occur for vegetation with the region (Konecky *et al.*,
238 2014).

239

240 The zonal plot of ethanol shows their highest levels at 30°N-60°N (up to 100 ppt), likely
241 due to larger anthropogenic emissions and at 15°S-15°N (up to 60 ppt) due to the
242 vegetation and biomass burning activity occurring within this region (Fig. 2). The
243 highest observed altitude (9.2 km) with significant ethanol concentrations (up to 30 ppt)
244 is found at 50°N-60°N during J-J-A and 60°N-90°N during D-J-F. Asian pollution
245 plumes could be contributing towards these levels which rise up into the upper
246 troposphere and transport towards Europe (Stohl *et al.*, 2007). There is less ethanol
247 present at the equator during J-J-A compared with D-J-F, which is likely to be due to
248 OH oxidation dominating as there is a large amount of sunlight within this region which
249 speeds up the reaction.

250

251 Figure 3 shows the ethanol observation flight data compilation of Naik *et al.* (2010)
252 along with simulated values produced by STOCHEM-CRI for the INTEX-NA
253 campaign conducted in July to August 2004 over eastern USA, INTEX-B campaign
254 conducted from February to April 2001 over the Gulf of Mexico, TRACE-P campaign

255 conducted in March 2001 over the North Pacific, and PEM-Tropics B campaign
256 conducted in March to April 1999 over the South Pacific. The model for all four
257 simulations exhibits an overall similar trend to the observed data, but the mixing ratios
258 of ethanol in the base case have been under predicted considerably in each case. The
259 vertical profile in Figure 3 shows a significant increase in ethanol when the extended
260 vegetation strength and anthropogenic contribution of ethanol is included (Run 2 and
261 3) which brings an improvement of the model in eastern USA, Gulf of Mexico and
262 South Pacific. Pollution from Asia that flows downward towards the Pacific could be
263 responsible for the higher levels of observed ethanol in North Pacific (Stohl *et al.*,
264 2007). A trend of increasing atmospheric concentration of ethanol with altitude over
265 the South Pacific is likely due to convective activity within this region taking pollutants
266 up with it via frontal lifting. The observational errors are relatively higher for all cases,
267 creating a large uncertainty into atmospheric ethanol levels throughout the troposphere,
268 which is due to periodic variations in ethanol emissions and weather phenomena. The
269 difference between the observed and modelled ethanol for all flight campaign data lie
270 within their respective standard deviation. However, the emission class data for the
271 model can be improved by incorporating updated biofuel emissions which could
272 improve the discrepancies between model and observed data.

273

274 Monthly surface model ethanol data was extracted for twenty stations around the globe
275 (Table 3) and then compared with measured ethanol data to evaluate the accuracy of
276 the model (Figure 4). The model ethanol simulated levels from the base case is largely
277 underestimated compared with the measured ethanol for all stations, which may be due
278 to the missing sources (e.g. vegetation) or the underestimating of the biofuel emission
279 in the simulation. The inclusion of vegetation and extended anthropogenic emissions in
280 the model (Run 2) give a better agreement between model and measured ethanol for
281 clean marine and remote environment (e.g. Central Gulf, Masonoro Island, Mace Head,
282 Trinidad Head, and NEAQS).

283

284 The addition of extended vegetation and oceanic emissions (Run 3) has produced a
285 huge improvement between model-measurement discrepancies of ethanol for the rural
286 environment (e.g. Wank, Jungfraujoeh, Santa Rita and Mt. Lemmon, Pennsylvania,
287 Nashville). The errors associated with the measured data of Chebogue Point, High
288 Arctic, Pittsburg, Wank, Santa Rita and Mt. Lemmon are significantly high, but with

289 the modelled data lying within one standard deviation of the mean suggesting the
290 difference is insignificant. The measured ethanol level at Houston and Galveston Bay
291 is much higher than the model ethanol values because the measurement site is close to
292 the downtown Houston making the site well within the urban corridor and the emission
293 of ethanol from this site is from anthropogenic sources which were heavily influenced
294 by industrial emissions (Gilman *et al.*, 2009). Granite Bay, CA is close to the
295 Sacramento urban area and two major highways and one gasoline refiner supplying fuel
296 to the Sacramento area used ethanol instead of methyl-t-butyl-ether during the
297 measurement year (Rubin *et al.*, 2006). The underprediction of ethanol by the model at
298 Houston and Galveston Bay and Granite bay is likely due to the level of anthropogenic
299 emissions being much greater than model used but also due to the resolution of
300 STOCHEM as volume averaging is occurring over such a large scale.

301

302 All urban areas (e.g. London, Porto Alegre, Osaka, Mexico City, Pittsburgh, Zurich)
303 show a very large deviation from the simulated concentrations of ethanol likely due to
304 the low resolution of STOCHEM ($5^{\circ} \times 5^{\circ}$) making it difficult to accurately model highly
305 polluted urban areas which make up only a small fraction of the grid. However due to
306 the large difference in magnitude it is likely that there is a source of ethanol currently
307 being under estimated or not being accounted for, suggesting primarily that
308 anthropogenic emissions (e.g. biofuel) are likely to be much larger than current
309 estimations. The observed ethanol in Porto Alegre are found to be higher than other
310 urban areas due to their use of ethanol fuel in cars. Osaka is a region in where ethanol
311 was not used as a biofuel in the measurement time and showed an observed
312 concentration that was much lower than Porto Alegre. Nguyen *et al.* (2001) study was
313 conducted on a main road through the Osaka city where ethanol may be emitted from
314 some other anthropogenic sources. The industrial and vehicle emissions are the main
315 sources of VOCs in two large metropolitan cities, London and Mexico City. The biofuel
316 has been becoming popular in both UK and Mexico in recent years due to positive
317 impacts on air quality. The UK's gasoline currently contains 5% ethanol and the value
318 is likely to be double by 2020 (Dunmore *et al.*, 2016). The underestimation of the
319 biofuel in the model makes the large discrepancies between measured and modelled
320 ethanol levels in Mexico City and London. There is a large variation in the measured
321 ethanol mixing ratios at two stations (e.g. Jungfaujoch and Zürich) of Switzerland

322 because Jungfaujoch is located at the 3580 m above from the sea level and has no nearby
323 anthropogenic emission sources, but Zürich is an urban background site which has
324 different nearby anthropogenic OVOC emissions from gasoline and solvent
325 evaporation, residential heating and small industrial enterprises. Higher levels of
326 observed ethanol at both stations of Switzerland in the winter are found which may due
327 to the temperature inversions occurring within the winter months, causing stagnant air
328 pollution to build up. Legreid *et al.* (2007) suggested that 55% of produced ethanol was
329 from combustion in summer as opposed to 41% in the winter, but levels of ethanol are
330 found to be lower in summer due to dominating of the removal processes.

331

332 The percentage change of surface mixing ratios of acetaldehyde, PAN and ozone from
333 base (Run 1) to Naik *et al.* (2010) emission scenario (Run 2) and from base to Kirstine
334 and Galbally (2012) emission scenario (Run 3) are shown in Figure 5. The mean surface
335 acetaldehyde mixing ratios have increased by up to 30% in Brazil, Australia and New
336 Guinea after adding vegetation and extended anthropogenic emission (Figure 5a).
337 Further increasing the vegetation and oceanic emissions has resulted in the increment
338 of acetaldehyde up to 90% in equatorial remote region and also in Brazil and New
339 Guinea (Figure 5b). Acetaldehyde is the dominating precursor of the formation of PAN
340 (Fischer *et al.*, 2014), thus an increment of PAN up to 3% from Run 1 to Run 2 (Figure
341 5c) and up to 10% from Run 1 to Run 3 (Figure 5d) was found over the ocean near
342 acetaldehyde source regions. The increases in ozone are driven by the redistribution of
343 NO_x (decomposition products of PAN) which is found to be largest in remote oceanic
344 regions (Figure 5e). The greatest percentage change up to 0.4% (Run 1 to Run 2) and
345 1.4% (Run 1 to Run 3) in ozone concentration is found at the surface over the tropical
346 oceans suggested that upon including vegetation and extended anthropogenic and
347 oceanic emissions of ethanol has led to a pronounced effect of the ozone chemistry in
348 this region.

349

350 CONCLUSION

351 In this paper, we used STOCHEM-CRI, a global 3-dimensional chemistry transport
352 model to capture the global distribution and seasonal cycle of ethanol. The global
353 burden of ethanol was found to be in between 0.024-0.25 Tg, matching well with
354 literature. The lifetime of ethanol is 1.1-2.8 days, thus a large amount of ethanol can be
355 transported from the continental boundary layer into the free troposphere which will

356 have a potentially significant impact on the concentration of oxidants. The
357 photochemical source of ethanol appeared to be lower limit in the study because of the
358 lack of the larger peroxy radical species and their corresponding rate constants in the
359 model. Globally there are significantly higher concentrations of ethanol modeled over
360 Saudi Arabia and Eastern Canada. The highest level of ethanol is modelled at 30°N-
361 60°N and 15°S-15°N. Overall STOCHEM-CRI has under predicted the concentration
362 of ethanol in most of the stations and flight campaigns discussed in the study. The
363 addition of vegetation and extended anthropogenic emissions in the model reduce the
364 discrepancies between modelled and measured ethanol concentrations. The area best
365 modelled using STOCHEM was the marine clean and rural areas was likely due to these
366 area being subject to insignificant amounts of anthropogenic emissions. The values
367 simulated are much lower than observed data for urban areas which could be due to the
368 level of anthropogenic emissions being much greater than used in the model but also
369 due to the resolution of STOCHEM making the areas harder to model accurately as the
370 emissions are measured over such a vast area. The model ethanol level of all flight
371 campaigns lie within one standard deviation of the mean suggesting the difference
372 between model and measurement is insignificant. The addition of ethanol has increased
373 within recent years; the worldwide with global production for 2020 estimated to be over
374 125 billion litres, compared with only 17.3 billion litres in 2000 (Balat and Balat, 2009).
375 The increasing use of biofuels globally will have an impact in the production of ozone
376 as well as hydroxyl radicals in the remote regions.

377

378

379

380 **ACKNOWLEDGEMENTS**

381 We thank NERC and Bristol ChemLabS under whose auspices various aspects of this
382 work were carried out. We also thank Prof. Michael Davies-Coleman for his valuable
383 suggestions during the preparation of the manuscript.

384

385

386

387

388

389

390 **References**

391 ATKINSON, R., BAULCH, D.L., COX, R.A., CROWLEY, J.N., HAMPSON, R.F.,
392 HYNES, R.G., JENKIN, M.E., ROSSI, M.J. & TROE, J. 2006. Evaluated kinetic and
393 photochemical data for atmospheric chemistry: volume II- gas phase reactions of
394 organic species. *Atmospheric Chemistry and Physics* 6: 3625–4055.

395

396 AVERY JR., G.B., FOLEY, L., CARROLL, A.L., ROEBUCK JR., J.A., GUY, A.,
397 MEAD, R.N., KIEBER, R.J., WILLEY, J.D., SKRABAL, S.A., FELIX, J.D.,
398 MULLAUGH, K.M. & HELMS, J.R. 2016. Surface waters as a sink and source of
399 atmospheric gas phase ethanol. *Chemosphere* 144: 360–365.

400

401 BALAT, M. & BALAT, H. 2009. Recent trends in global production and utilization
402 of bio-ethanol fuel. *Applied Energy* 86: 2273–2282.

403

404 BLANDO, J.D. & TURPIN, B.J. 2000. Secondary organic aerosol formation in cloud
405 and fog droplets: A literature evaluation of plausibility. *Atmospheric Environment* 34:
406 1623–1632.

407

408 BOUDRIES, H., BOTTENHEIM, J.W., GUIMBAUD, C., GRANNAS, A.M.,
409 SHEPSON, P.B., HOUDIER, S., PERRIER, S. & DOMINÉ, F. 2002. Distribution
410 and trends of oxygenated hydrocarbons in the high Arctic derived from measurements
411 in the atmospheric boundary layer and interstitial snow air during the ALERT2000
412 field campaign. *Atmospheric Environment* 36: 2573–2583.

413

414 COLLINS, W.J., STEVENSON, D.S., JOHNSON, C.E. & DERWENT, R.G., 1997.
415 Tropospheric ozone in a Global-Scale Three-Dimensional Lagrangian Model and its
416 response to NO_x emission controls. *Journal of Atmospheric Chemistry* 26: 223–274.

417

418 DERWENT, R.G., STEVENSON, D.S., DOHERTY, R.M., COLLINS, W.J. &
419 SANDERSON, M.G. 2008. How is surface ozone in Europe linked to Asian and
420 North American NO_x emissions? *Atmospheric Environment* 42: 7412–7422.

421

422 DUNMORE, R.E., WHALLEY, L.K., SHERWEN, T., EVANS, M.J., HEARD, D.E.,
423 HOPKINS, J.R., LEE, J.D., LEWIS, A.C., LIDSTER, R.T., RICKARD, A.R. &
424 HAMILTON, J.F. 2016. Atmospheric ethanol in London and the potential impacts of
425 future fuel formulations. *Faraday Discussions* (in Press).

426

427 FEHSENFELD, F., CALVERT, J., FALL, R., GOLDAN, P., GUENTHER, A.B.,
428 HEWITT, C.N., LAMB, B., LIU, S., TRAINER, M., WESTBERG, H. &
429 ZIMMERMAN, P. 1992. Emissions of volatile organic compounds from vegetation
430 and the implications for atmospheric chemistry. *Global Biogeochemical Cycles* 6:
431 389–430.

432

433 FISCHER, E.V., JACOB, D.J., YANTOSCA, R.M., SULPRIZIO, M.P., MILLET,
434 D.B., MAO, J., PAULOT, F., SINGH, H.B., ROIGER, A., RIES, L., TALBOT, R.W.,
435 DZEPINA, K. & DEOLAL, S.P. 2014. Atmospheric peroxyacetyl nitrate (PAN): a
436 global budget and source attribution. *Atmospheric Chemistry and Physics* 14:
437 2679–2698.

438

- 439 GARZÓN, J.P., HUERTAS, J.I., MAGAÑA, M., HUERTAS, M.E., CÁRDENAS,
440 B., WATANABE, T., MAEDA, T., WAKAMATSU, S. & BLANCO, S. 2015.
441 Volatile organic compounds in the atmosphere of Mexico City. *Atmospheric*
442 *Environment* 119: 415-429.
- 443
444 GILMAN, J.B., KUSTER, W.C., GOLDAN, P.D., HEMDON, S.C., ZAHNISER,
445 M.S., TUCKER, S.C., BREWER, W.A., LERNER, B.M., WILLIAMS, E.J.,
446 HARLEY, R.A., FEHSENFELD, F.C., WARNEKE, C. & DE GOUW, J.A. 2009.
447 Measurements of volatile organic compounds during the 2006 TexAQS/GoMACCS
448 campaign: Industrial influences, regional characteristics, and diurnal dependencies of
449 the OH reactivity. *Journal of Geophysical Research* 114: D00F06.
- 450
451 GROSJEAN, E., RASMUSSEN, R.A. & GROSJEAN, D. 1998. Ambient levels of
452 gas phase pollutants in porto alegre, Brazil. *Atmospheric Environment* 32:
453 3371–3379.
- 454
455 GRANIER, C., LAMARQUE, J.F., MIEVILLE, A., MULLER, J.F., OLIVIER, J.,
456 ORLANDO, J., PETERS, J., PETRON, G., TYNDALL, S. & WALLENS, S. 2005.
457 POET, a database of surface emissions of ozone precursors,
458 http://accent.aero.jussieu.fr/database_table_inventories.php (accessed 5 July 2016)
- 459
460 GUENTHER, A.B., JIANG, X., HEALD, C.L., SAKULYANONTVITTAYA, T.,
461 DUHL, T., EMMONS, L.K. & WANG, X. 2012. The Model of Emissions of gases
462 and Aerosols from nature version 2.1 (MEGAN2.1): an extended and updated
463 framework for modelling biogenic emissions. *Geoscientific Model Development* 5:
464 1471–1492.
- 465
466 JACOBSON, M.Z. 2007. Effects of ethanol (E85) versus gasoline vehicles on cancer
467 and mortality in the United States. *Environmental Science and Technology* 41:
468 4150–4157.
- 469
470 JENKIN, M.E., WATSON, L.A., UTEMBE, S.R. & SHALLCROSS, D.E. 2008. A
471 Common Representative Intermediate (CRI) mechanism for VOC degradation. Part-1:
472 gas phase mechanism development. *Atmospheric Environment* 42: 7185–7195.
- 473
474 JOSÉ, G. 2013. Sugarcane Ethanol: Strategies to a successful program in Brazil. In
475 LEE, J.W (Ed.) *Advanced biofuels and bioproducts*. Springer-Verlag New York, pp.
476 13–20.
- 477
478 KIRSTINE, W.V. & GALBALLY, I.E. 2012. The global atmospheric budget of
479 ethanol revisited. *Atmospheric Chemistry and Physics* 12: 545–555.
- 480
481 KONECKY, B., RUSSELL, J., HUANG, Y., VUILLE, M., COHEN, L. & STREET-
482 PERROTT, F.A. 2014. Impact of monsoons, temperature and CO₂ on the rainfall and
483 ecosystems of Mt. Kenya during the Common Era. *Palaeogeography*
484 *Palaeoclimatology Palaeoecology* 396: 17–25.
- 485
486 LEGREID, G., LÖÖV, J.B., STAEHELIN, J., HUEGLIN, C., HILL, M.,
487 BUCHMANN, B., PREVOT A.S.H. & REIMANN, S. 2007. Oxygenated volatile

- 488 organic compounds (OVOCs) at an urban background site in Zürich (Europe):
489 seasonal variation and source allocation. *Atmospheric Environment* 41: 8409–8423.
490
- 491 LEGREID, G., FOLINI, D., STAEHELIN, J., LÖÖV, J.B., STEINBACHER & M.,
492 REIMANN, S. 2008. Measurements of organic trace gases including oxygenated
493 volatile organic compounds at the alpine site Jungfrauoch (Switzerland): seasonal
494 variation and source allocation. *Journal of Geophysical Research* 113: D05307.
495
- 496 LEIBROCK, E. & SLEMR, J. 1997. Method for measurement of volatile oxygenated
497 hydrocarbons in ambient air. *Atmospheric Environment* 31: 3329–3339.
498
- 499 MILLET, D.B., GOLDSTEIN, A.H., ALLAN, J.D., BATES, T.S., BOUDRIES, H.,
500 BOWER, K.N., COE, H., MA, Y., MCKAY, M., QUINN, P.K., SULLIVAN, A.,
501 WEBER, R.J. & WORSNOP, D.R. 2004. Volatile organic compound measurements
502 at Trinidad Head, California, during ITCT 2K2: Analysis of sources, atmospheric
503 composition, and aerosol residence times. *Journal of Geophysical Research* 109:
504 D23S16.
505
- 506 MILLET, D.B., DONAHUE, N.M., PANDIS, S.N., POLIDORI, A., STANIER, C.O.,
507 TURPIN, B.J. & GOLDSTEIN, A.H. 2005. Atmospheric volatile organic compound
508 measurements during the Pittsburgh Air Quality Study: Results, interpretation, and
509 quantification of primary and secondary contributions. *Journal of Geophysical*
510 *Research* 110: D07S07.
511
- 512 MILLET, D.B., GOLDSTEIN, A.H., HOLZINGER, R., WILLIAMS, B.J., ALLAN,
513 J.D., JIMENEZ, J.L., WORSNOP, D.R., ROBERTS, J.M., WHITE, A.B.,
514 HUDMAN, R.C., BERTSCHI, I.T. & STOHL, A. 2006. Chemical characteristics of
515 North American surface layer outflow: insights from Chebogue point, Nova Scotia.
516 *Journal of Geophysical Research* 111: D23S53.
517
- 518 MILLET, D.B., GUENTHER, A., SIEGEL, D.A., NELSON, N.B., SINGH, H.B., DE
519 GOUW, J.A., WARNEKE, C., WILLIAMS, J., EARDEKENS, G., SINHA, V.,
520 KARL, T., FLOCKE, F., APEL, E., RIEMER, D.D., PALMER, P.I., BARKLEY, M.
521 2010. Global atmospheric budget of acetaldehyde: 3-D model analysis and constraints
522 from in-situ and satellite observations. *Atmospheric Chemistry and Physics* 10:
523 3405–3425.
524
- 525 MILLET, D.B., APEL, E., HENZE, D.K., HILL, J. MARSHALL, J.D., SINGH, H.B.
526 & TESSUM, C.W. 2012. Natural and Anthropogenic ethanol sources in North
527 America and potential atmospheric impacts of ethanol fuel use. *Environmental*
528 *Science and Technology* 46: 8484–8492.
529
- 530 MURPHY, J.G., DAY, D.A., CLEARY, P.A., WOOLDRIDGE, P.J., MILLET, D.B.,
531 GOLDSTEIN, A.H. & COHEN, R.C. 2007. The weekend effect within and
532 downwind of Sacramento-Part 1: observations of ozone, nitrogen oxides, and VOC
533 reactivity. *Atmospheric Chemistry and Physics* 7: 5327–5339.
534
- 535 NAIK, V., FIORE, A.M., HOROWITZ, L.W., SINGH, H.B., WIEDINMYER, C.,
536 GUENTHER, A., DE GOUW J.A., MILLET, D.B., GOLDAN, P.D., KUSTER, W.C.

- 537 & GOLDSTEIN, A. 2010. Observational constraints on the global atmospheric
538 budget of ethanol. *Atmospheric Chemistry and Physics* 10: 5361–5370.
539
- 540 NGUYEN, H.T-H., TAKENAKA, N., BANDOW, H., MAEDA, Y., DE OLIVA,
541 S.T., BOTELHO, M.M.f. & TAVARES, T.M. 2001. Atmospheric alcohols and
542 aldehydes concentrations measured in Osaka, Japan and in Sao Paulo, Brazil.
543 *Atmospheric Environment* 35: 3075–3083.
544
- 545 RIEMER, D., POS, W., MILNE, P., FARMER, C., ZIKA, R., APEL, E., OLSZYNA,
546 K., KLIENDIENST, T., LONNEMAN, W., BERTMAN, S., SHEPSON, P. &
547 STARN, T. 1998. Observations of nonmethane hydrocarbons and oxygenated volatile
548 organic compounds at a rural site in the southeastern United States. *Journal of*
549 *Geophysical Research* 103: 28111–28128.
550
- 551 RUBIN, J.I., KEAN, A.J., HARLEY, R.A., MILLET, D.B. & GOLDSTEIN, A.H.
552 2006. Temperature dependence of volatile organic compound evaporative emissions
553 from motor vehicles. *Journal of Geophysical Research* 111: D03305.
554
- 555 SANDER, R. 2015. Compilation of Henry's law constants (version 4.0) for water as
556 solvent. *Atmospheric Chemistry and Physics* 15: 4399–4981.
557
- 558 SINGH, H.B., SALAS, L., CHATFIELD, R., CZECH, E., FRIED, A., WALEGA, J.,
559 EVANS, M., FIELD, B., JACOB, D., BLAKE, D., HEIKES, B., TALBOT, R.,
560 SACHSE, G., CRAWFORD, J., AVERY, M., SANDHOLM, S. & FUELBERG, H.
561 2004. Analysis of the atmospheric distribution, sources and sinks of oxygenated
562 volatile organic chemicals based on measurements of the Pacific during TRACE-P.
563 *Journal of Geophysical Research* 109: D15S07.
564
- 565 SNIDER, J.R. & DAWSON, G.A. 1985. Tropospheric light alcohols, carbonyls and
566 acetonitrile: concentrations in the southwestern United States and Henry's law data.
567 *Journal of Geophysical Research* 90: 3797–3805.
568
- 569 STOHL, A., FORSTER, C., HUNTRIESER, H., MANNSTEIN, H., MCMILLAN,
570 W.W., PETZOLD, A., SCHLAGER, H. & WEINZIERL, B. 2007. Aircraft
571 measurements over Europe of an air pollution plume from Southeast Asia-aerosol and
572 chemical characterization. *Atmospheric Chemistry and Physics* 7: 913–937.
573
- 574 SUAREZ-BERTOIA, R., ZARDINI, A.A., KEUKEN, H. & ASTORGA, C. 2015.
575 Impact of ethanol containing gasoline blends on emissions from a flex-fuel vehicle
576 tested over the Worldwide Harmonized Light duty Test Cycle (WLTC). *Fuel* 143:
577 173–182.
578
- 579 SUNDVOR, I. & LÓPEZ-APARICIO, S. 2014. Impact of bioethanol fuel
580 implementation in transport based on modelled acetaldehyde concentration in the
581 urban environment. *Science of the Total Environment* 496: 100–106.
582
- 583 UTEMBE, S.R., COOKE, M.C., ARCHIBALD, A.T., JENKIN, M.E., DERWENT,
584 R.G. & SHALLCROSS, D.E. 2010. Using a reduced Common Representative
585 Intermediates (CRI v2-R5) mechanism to simulate tropospheric ozone in a 3-D
586 Lagrangian chemistry transport model. *Atmospheric Environment* 13: 1609–1622.

- 587
588 WALSH, R.C. 2010. High frequency observations and analysis of OVOCs using Gas
589 Chromatography-Mass Spectrometry. Unpublished PhD thesis. University of Bristol,
590 UK.
- 591
592 WARNEKE C., KATO, S., DE GOUW, J.A., GOLDAN, P.D., KUSTER, W.C.,
593 SHAO, M., LOVEJOY, E.R., FALL, R. & FEHSENFELD, F.C. 2005. Online volatile
594 organic compound measurements using a newly developed proton-transfer ion-trap
595 mass spectrometry instrument during New England Air Quality Study-Intercontinental
596 Transport and Chemical Transformation, 2004. Performance, intercomparison, and
597 compound identification. *Environmental Science and Technology* 39: 5390–5397.
- 598
599 WATSON, L.A., SHALLCROSS, D.E., UTEMBE, S.R. & JENKIN, M.E. 2008. A
600 Common Representative Intermediate (CRI) mechanism for VOC degradation. Part 2:
601 gas phase mechanism reduction. *Atmospheric Environment* 42: 7196–7204.
602